Third International Conference on Biaxial/Multiaxial Fatigue

INFLUENCE OF INITIAL PLASTIC DEFORMATION IN WELD METAL ON FATIGUE CRACK GROWTH

J. Legat*, S. Sedmak**, B. Petrovski**

* - Technical High School, University of Maribor, Maribor, Yugoslavia
** - Faculty of Technology and Metallurgy, University of Belgrade, Belgrade, Yugoslavia

ABSTRACT

The welded testpieces, obtained by gas-shielded welding of NIONIKRAL 70 steel (low-alloyed Ni-Cr steel with 700 MPa yield strength and 800 MPa ultimate tensile strength) were exposed to tensile loading in order to produce initial plastic strain of the desired level in the weld metal.The three point bending specimens for the fatique crack growth testing have been machined out from the plastically deformed testpieces, with the notch tip positioned in the middle of the weld metal. Crack length during the fatigue was evaluated accordingly to the slope in the load-COD relationship (compliance), taken after a given number of cycles of the applied load. Crack growth rate has been determined from the a vs. N plots (a-crack length, N-number of cycles), while the stress intensity factor range ΔK has been calculated using the formulae from ASTM E399. It has been found that the level of the initial plastic strain affects both the coefficient C and the exponent n in the Paris' law $da/dN=C\cdot\Delta K^n$.

INTRODUCTION

Successful application of welded structures depends in many cases on welded joints ability to sustain complex variable loadings, in critical situations combined with monotonicaly raising overloadings. This is very important when the welded structure is produced of high strength steel, that enables significant reduction of material consume compared to low strength steel. Pressure vessels, penstocks and pipe-lines represent examples when weldable high-strength steels of 700 MPa yield strength have already been applied. Steelworks "Jesenice" in Yugoslavia produces weldable NIONIKRAL 70 steel of this strength level, exhibiting low transition temperature in addition to good strength and toughness properties [1].

It has been found [2] that in welded structures, exposed to the inner pressure, yield strength could be locally achieved due to stress concentration in welded joints. The plastic strain will be developed in this situation in weld metal or in base metal in accordance with matching and hardening properties of both base and weld metals. Acting codes and rules require proof presurizing up to 50% higher pressure compared to design pressure, and in combination with welding residual stresses this can easily produce significant amount of locally developed plastic deformation. In some service conditions variable pressure can be introduced after initial plastic deformation and the response of plastically strained welded joint constituents can govern the overall mechanical behaviour of pressure vessel or similar structure. Structural heterogeneity of weldments indicates weld metal as critical part due to cast microstructure and heat-affected-zone (HAZ) due to differently structured portions [3]. Cracks or crack-like defects are inevitably contained in these two weldment constituents and this situation requires the analysis of crack growth behaviour under variable loading. Weld metal could be a critical constituent when fatigue crack growth is considered. For this reason, fatigue crack growth has been experimentally analyzed after initial plastic deformation in weld metal of high-strength NIONIKRAL 70 steel.

SAMPLES AND TESTPIECES PREPARING

The NIONIKRAL 70 steel, with chemical composition given in Table 1, is used for this experiment. The samples of welded joints had been prepared by CO_2 gas shielded welding, using ϕ 1.2 wire FLUXOFIL 42, produced by "Jesenice". Preheating temperature of 120°C had been required.

Table 1. Chemical composition of NIONIKRAL 70 steel (%)

C	Si	Mn	Cr	Ni	Mo	P	S
0.14	0.36	1.02	0.99	2.61	0.30	0.013	0.003

The shape of welded samples is presented in Fig. 1.

Tensile properties had been determined on the specimens, presented in Fig. 2. This type of specimens had been used in experiments with NIONIKRAL 70 steel and its welded joints [4] for determination of S-N relationship according to ASTM E647 [5]. Proof yield strength $R_{p0,2}$ and ultimate tensile strength R_m (Table 2) have been determined from typical results of tensile test, presented in Fig. 3.

Table 2. Tensile properties of NIONIKRAL 70 steel and its weldment (CO_2 gas shielded welding)

Specimen from	Proof yield strength $R_{p0,2}$, MPa	Ultimate tensile strength R_m, MPa
a. base metal, rolling direction	692	783
b. base metal, cross-rolling direction	612	801
c. welded joint	690	802

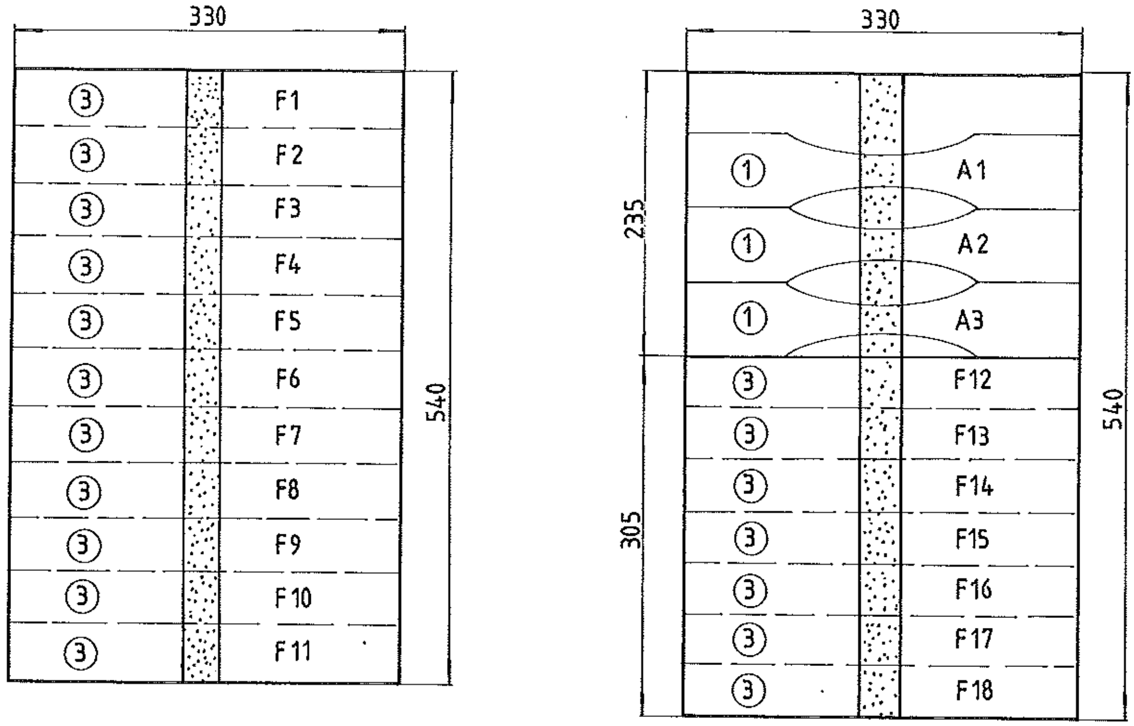

Figure 1. Welded samples with specimens disposition

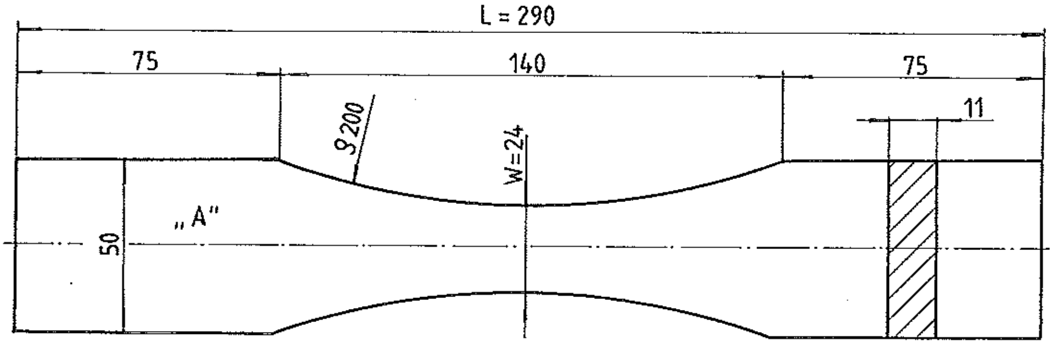

Figure 2. Tensile specimens, made of base metal and welded joint

It is to be mentioned that displacement in welded joint specimen is presented only as an average of base metal (including HAZ) and weld metal displacement, measured by an extensometer with nominal length of 50 mm. One can conclude from Fig. 3 that strain distribution during tension depends not only on yield strength level, but on the hardening properties of base and weld metal as well.

Tensile test results have shown that slightly overmatched weld metal has been obtained in this welded joint, but the behaviour of weld metal can not be completely described from relationship presented in Fig. 3c. The application of strain gauges, distributed in a proper way on typical regions of specimen,

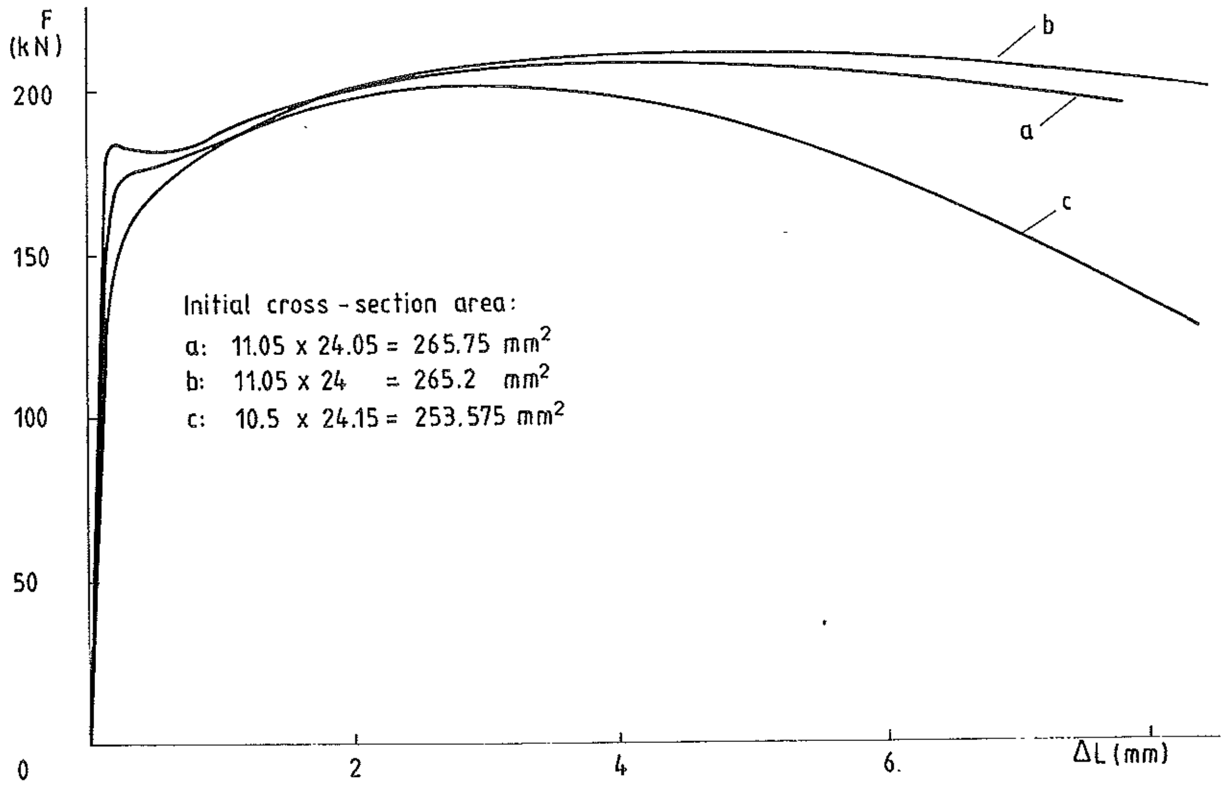

Figure 3. Load F vs. average elongation ΔL for NIONIKRAL 70 steel in rolling direction (a) and cross rolling direction (b), and for welded joint (c)

can help in description of heterogenious deformation of welded joint [3,6]. However, from the comparison of Fig. 3a and 3c one can conclude that yield strength level is achieved in weld metal first. The weldment is positioned normally to rolling direction of base metal. Accordingly, weld metal started to yield first in this welded joint. The hardening capacity of weld metal directed the plastic deformation from weld metal to base metal, where the specimen was finally broken.

The welded joint specimens, shaped according to Fig. 4, had been equiped by supporting knives with 5 mm edge distances for an application of crack-opening-displacement (COD) gauge, usually applied in fracture mechanics tests. In this way the deformation of weld metal could be approximatelly followed during the development of initial plastic deformation.

Data from Table 3 show that plastic strains in weld metal ranged between 0.053% and 0.874%. In most cases the plastic strains in base metal are higher than in weld metal, but in some specimens they are lower (e.g. F12, F2, F7). Such a behaviour could be attributed to the lower yield point and higher hardening capacity of weld metal compared to base metal in this region of strains.

Total amount of specimen plastic strain had been evaluated according to the displacement of measuring points, initially positioned on L_0=100 mm no-

Table 3. Initial deformation for differently strained weld metals.

Specimen	Maximal applied load	Measuring points distance: initial	Measuring points distance: after unloading	Elongation	Plastic deformation	Elastic deformation	Elastic elongation portion	Measuring base for COD gauge	Elongation measured on COD gauge	Plastic deformation of weld metal
	F_g	L_o	L_k	ΔL_o	ε_p	ε_e	δ_e	δ_o	δ	$\varepsilon_{p\delta}$
	kN	mm	mm	mm	%	%	µm	mm	µm	%
F6	213	99.87	103.144	3.274	3.28	0.368	55.2	15	128	0.853
F18	211	99.77	103.461	3.691	3.7	0.365	52.8	14.5	126.8	0.874
F11	208	98.65	100.505	1.855	1.88	0.361	78	21.6	100.8	0.467
F9	202	99.86	101.606	1.746	1.75	0.351	54.8	15.6	47.2	0.303
F13	200	99.95	101.426	1.476	1.48	0.347	53.2	15.3	55.2	0.361
F10	195	99.88	100.74	0.86	0.86	0.338	52.4	15.5	49.6	0.32
F12	192	100.5	100.058	0.06	0.06	0.333	95.2	28.5	31.2	0.109
F8	188	100.5	101.5	1.0	1.0	0.326	78.4	24.0	28.8	0.12
F3	186	99.82	100.074	0.254	0.25	0.323	54.4	16.8	34.4	0.205
F4	178	100.15	100.254	0.104	0.10	0.311	85.2	27.4	27.6	0.1
F5	171	99.658	99.255	0.097	0.1	0.296	66.8	22.6	12	0.053
F2	164	100.216	100.235	0.019	0.02	0.284	82.8	29.2	18.4	0.063
F2	158	100.213	100.254	0.041	0.04	0.274	54.4	19.3	11.2	0.056

minal distance, that were measured before and after straining on the table of precise coordinate drilling machine. During straining procedure, the relationship load - COD had been plotted (Fig. 5). Different maximal loads had been applied and different plastic strain levels of weld metals had been achieved (Table 3). The procedure of plastic strain evaluation is described for the specimen F3 (Fig. 5 and Table 3).

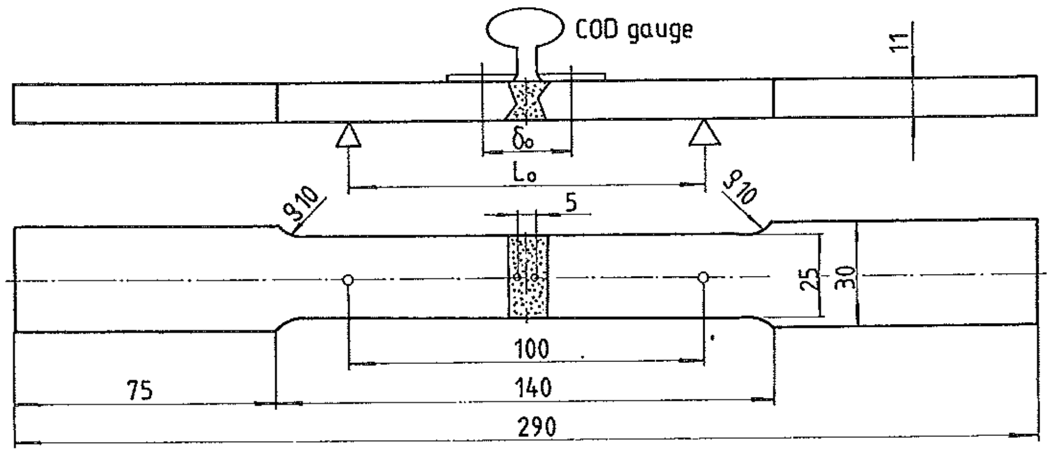

Figure 4. Welded joint specimen with mounted COD gauge for determination of initial plastic deformation in weld metal

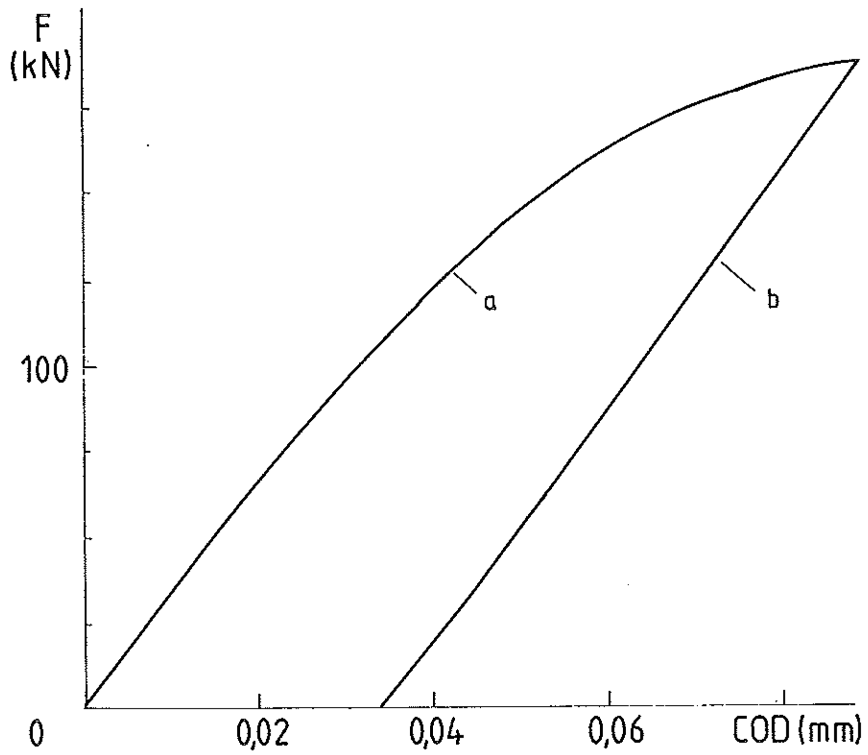

Figure 5. Relationship load F vs. COD, with gauge postioned in weld metal region during loading (a) and unloading (b)

When the required load level, determined in accordance with previous experience in experiment, had been achieved (F=186 kN for F3 specimen), the loading was interrupted and measuring point distance measured (L_k=100.074 mm). With initial distance L_o=99.82 mm, one can calculate the overall plastic deformation as:

$$\varepsilon_p = \frac{L_k - L_o}{L_o} = \frac{100.074-99.82}{99.82} = 0.25\%$$

The elastic strain could be evaluated from

$$\varepsilon_e = \frac{\sigma}{E} = \frac{F}{S_o E} = \frac{186\text{x}10^3}{10.97\text{x}25\text{x}210\text{x}10^3} = 0.323\%$$

with net section stress $\sigma = F/S_o$, load F=186 kN, cross-section area $S_o = B_o x W_o$= =10.97x25 mm², thickness B_o=10.97 mm and width W_o=25 mm, and elasticity modulus E=210 GPa. This elastic strain is accepted as representative for the range of COD gauge, because the E value is the same for both base and weld metals. But the range of COD readings can not be taken as the distance of knives edges; its initial value δ_o must be taken somewhere in the middle of bonded knives basis and COD extension has to be based on δ_o calculated value. Elastic strain portion in Fig. 5 corresponds to the straight unloading line, and one can read δ_e=54.4 μm. In this way the initial range δ_o for F3 specimen is

$$\delta_o = \frac{\delta_e}{\varepsilon_e} = \frac{54.4\text{x}10^{-3}}{0.323\text{x}10^{-2}} = 16.8 \text{ mm}$$

The measured plastic displacement was found to be δ_p=34.4 μm (Fig. 5) and the plastic strain of weld metal amounts to

$$\varepsilon_{p\delta} = \frac{\delta_p}{\delta_o} = \frac{34.4}{16.8}\frac{[\mu m]}{[mm]} = 0.00205 = 0.205\%$$

for the specimen F3.

SPECIMENS AND FATIGUE TESTING

After pre-straining of samples, the specimens for fatigue testing had been cut out according to Fig. 6. The shape of the specimen had been defined according to the experience gathered in previous fracture mechanics and fatigue tests. For specimen width of 25 mm the span has to be 100 mm according to ASTM E399 [7], and this enabled the application of variable loading to the

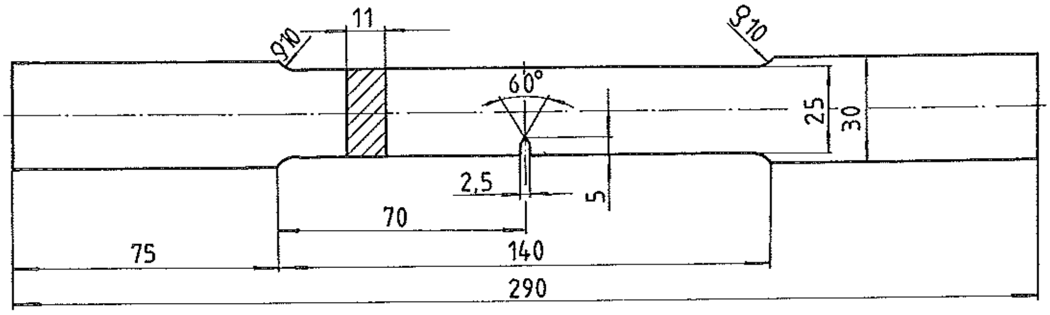

Figure 6. Three point bend specimen - SE (B) for fatigue crack growth analysis

original specimen shape, that means the initial overall length of the specimen had not be reduced. The original notch had been limited to approximately 20% of specimen width and the residual ligament was long enough for following crack growth in fatigue procedure.

The load range in one cycle

$$\Delta F = F_{max} - F_{min} = 8 - 0.8 = 7.2 \text{ kN}$$

had been accepted from the previous experiments with base metal specimens [4]. The frequency f = 50 Hz and ratio

$$R = \frac{F_{min}}{F_{max}} = 0.1$$

were applied for all specimens in this experiment.

Fatigue tests had been performed on Instron 1250 fatigue testing machine. The actual crack length had been evaluated from compliance, and according to testing program, the COD vs. load plots were drawn after specified cycle numbers (Fig. 7). This enabled the evaluation of crack length a from compliance slope EBC and specimen calibration (Fig. 8). In addition, actual crack length had been followed by an optical microscope with 25x magnification, on milimetric scale printed on the specimen side surface along the expected crack path. From the data in Fig. 7 the relationship crack length a vs cycle number N could be drawn (Fig. 9).

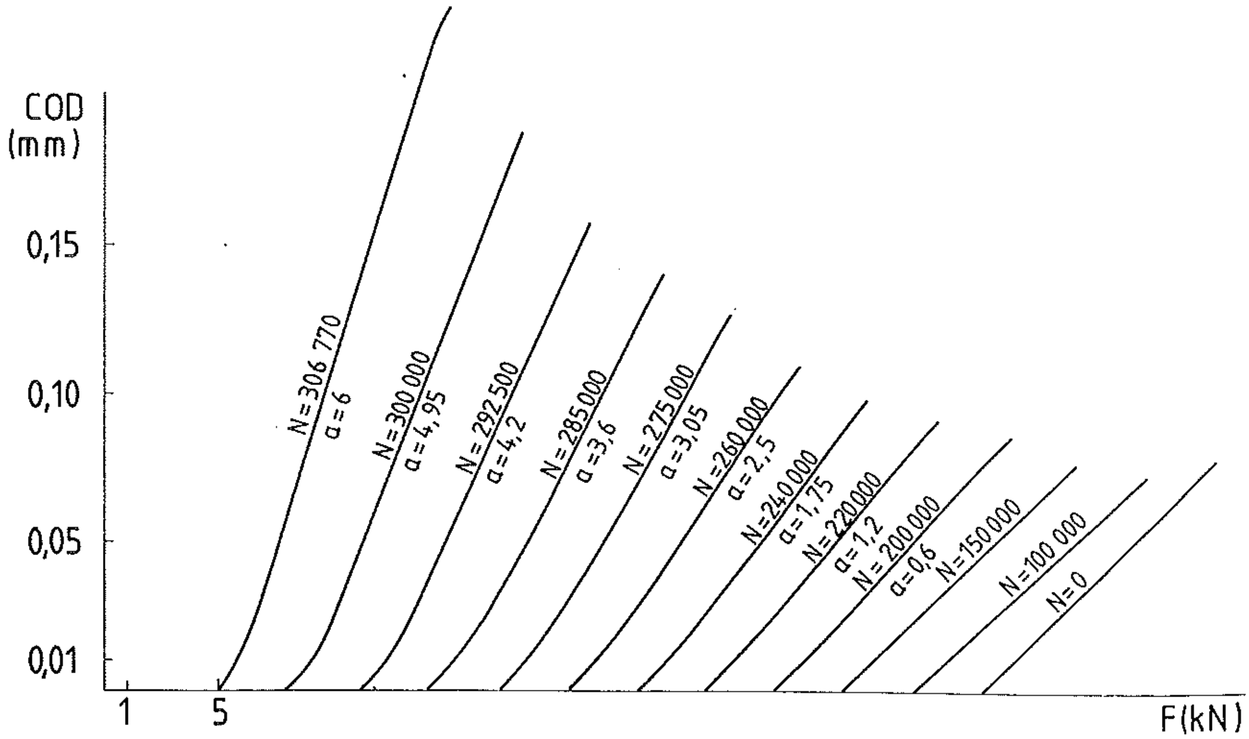

Figure 7. The change of compliance slope with growing cycle numbers N

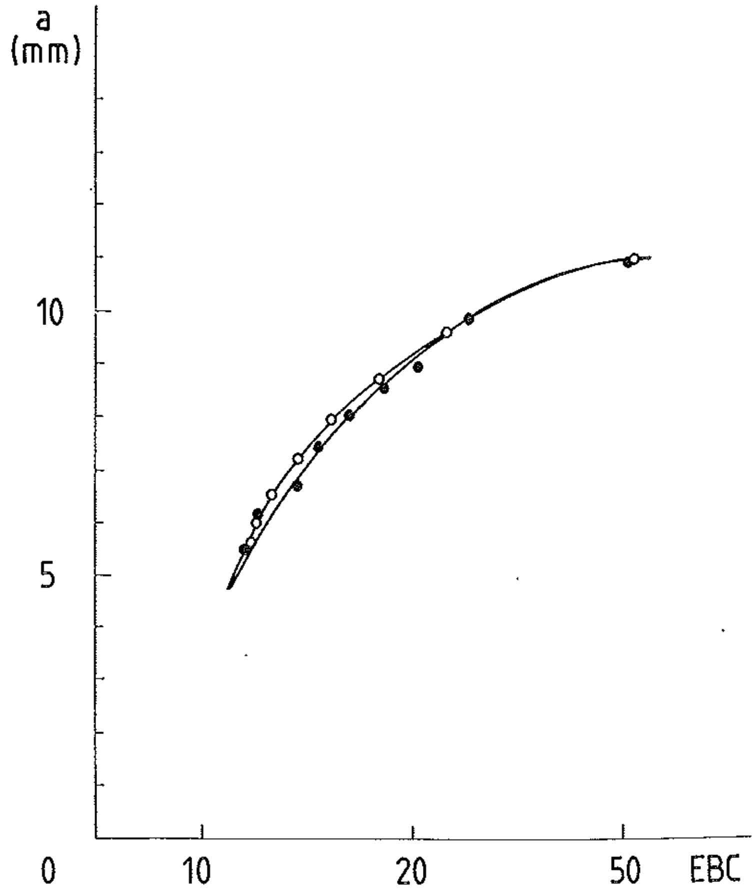

Figure 8. Experimentaly obtained SE (B) specimen compliance ECB calibration
for different crack length a

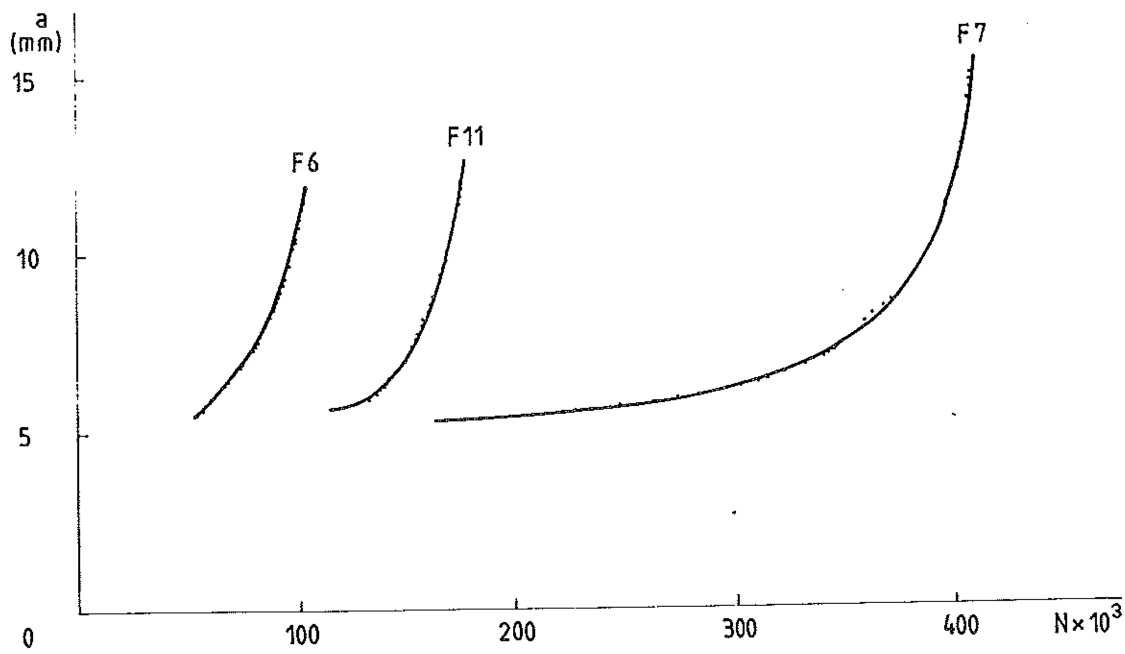

Figure 9. Relationship crack length a vs. cycle number N for specimens F6 (0.853% plastic pre-strain), F11 (0.467% plastic pre-strain) and F7 (0.056% plastic pre-strain)

ANALYSIS OF EXPERIMENTAL RESULTS

Experimentally obtained values for a-N pairs, ploted in Fig. 9 for typical specimens F6, F11 and F7 with different plastic pre-strain levels, had been used in procedure for da/dN values evaluation in a way explained in Fig. 10.

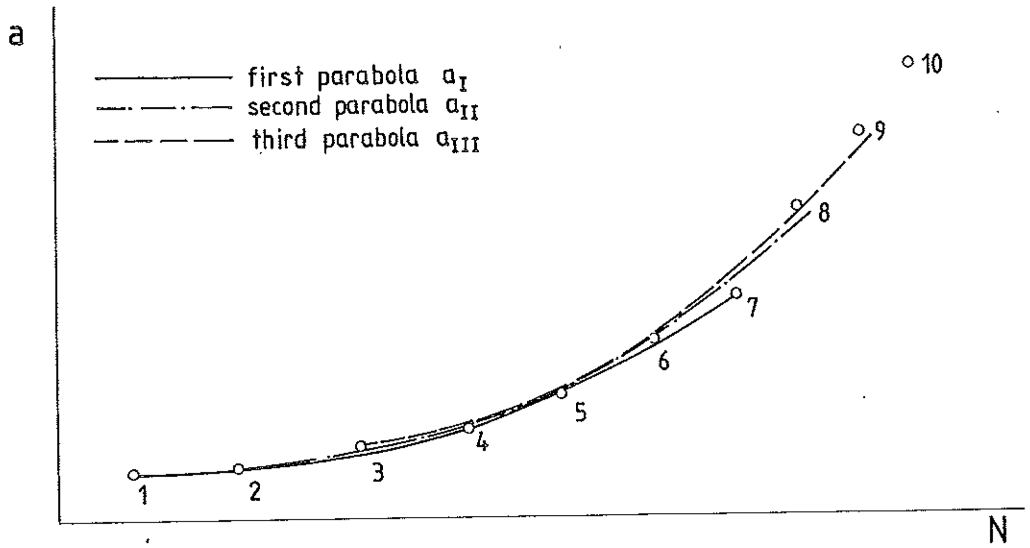

Figure 10. Selection of points for crack growth rate da/dN determination

Computer program defines parabolic equation

$$a_I = b_0 + b_1N + b_2N^2$$

through seven successive points, starting with first a-N pair, using standard deviation method. The first parabola is defined through points 1-7, the second through points 2-8 and so on. Crack growth rate is determined for point 4 in first parabola, for point 5 in the second, e.g.

$$\frac{da}{dN} = b_1 + 2b_2N$$

The applied approximation in da/dN can be considered as acceptable, having in mind the experimental approach in this examination.

Stress intensity factor range ΔK is required, in addition to da/dN, for the evaluation of coefficient C and exponent n in Paris law [8]

$$\frac{da}{dN} = C(\Delta K)^n$$

The stress intensity factor range is determined from [6]

$$\Delta K = \frac{\Delta F x L}{BW^{3/2}} \times f(\frac{a}{W})$$

with

$$f(\frac{a}{W}) = \frac{3(\frac{a}{W})^{1/2}[1.99 - \frac{a}{W}(1-\frac{a}{W})(2.15 - 3.93\frac{a}{W} + 2.7(\frac{a}{W})^2]}{2(1+2\frac{a}{W})(1-\frac{a}{W})^{3/2}}$$

where B=11 mm stands for specimen thickness, W=25 mm specimen width, a [mm] actual crack length, L=100 mm bending support span and ΔF=7.2 kN is load range.

The output from computer program is presented in Table 4 for F6 specimen as an example.

The results of this analysis are presented in Fig. 11-13 for different levels of initial plastic strain from Table 3.

DISCUSSION

The difference of slopes in Fig. 11 for two specimens with highest plastic pre-strain (F6 and F18) requires further consideration. It is clear from the diagram for F18 that ΔK values differ only slightly in the region of low crack growth rates. If they are supposed to belong to the region I of da/dN = f(ΔK) relationship [8], they have to be omitted from Paris law relation. The other points fall in the region of points obtained with F6 specimen. When only these points are taken for region II (Paris law), the obtained values $C = 2.2711 \times 10^{-9}$ and n = 2.63 are in the good agreement with corresponding values of F6 specimens.

Table 4. Crack growth rate da/dN and stress intensity factor range ΔK
(specimen F6 with initial plastic deformation 0.853%)

Dimensions: B = 11.0 mm W = 25.0 mm
Frequency f = 50 Hz
Temperature t = 20°C
Load: F_{min} = 0.800 kN
F_{max} = 8.000 kN

Point	Number of cycles N	Crack length measured a mm	Crack length aproximate mm	Stress intensity factor range ΔK MPa√m	Stress intensity factor range ΔK $N/mm^{3/2}$	Crack growth rate da/dN mm/kcykle
1	55600	5.600				
2	56700	5.700				
3	58000	5.800				
4	59050	5.900	5.889	21.364	675	.076
5	60500	6.000	5.965	21.534	680	.062
6	68100	6.400	6.421	22.564	713	.070
7	69350	6.500	6.499	22.745	719	.077
8	71900	6.700	6.706	23.229	734	.088
9	72880	6.800	6.806	23.468	742	.082
10	73900	6.900	6.890	23.668	748	.083
11	75100	7.000	6.984	23.898	755	.081
12	80900	7.400	7.410	24.960	789	.097
13	81880	7.510	7.510	25.215	797	.098
14	82800	7.600	7.601	25.452	804	.103
15	88200	8.300	8.276	27.288	862	.125
16	90200	8.500	8.532	28.027	886	.129
17	90730	8.600	8.603	28.237	892	.134
18	91500	8.700	8.696	28.514	901	.145
19	92170	8.800	8.803	28.838	911	.153
20	92800	8.900	8.896	29.121	920	.155
21	93450	9.00	8.998	29.438	930	.162
22	94700	9.200	9.206	30.102	951	.177
23	95180	9.300	9.297	30.395	961	.183
24	97250	9.700	9.709	31.783	1005	.207
25	99400	10.200	10.186	33.503	1059	.212
26	100350	10.400	10.390	34.277	1083	.223
27	100850	10.500	10.502	34.713	1097	.233
28	102350	10.800	10.842	36.090	1141	.256
29	102900	11.000				
30	103580	11.200				
31	104660	11.500				

$C = 1.5098 \times 10^{-9}$

$n = 2.698$

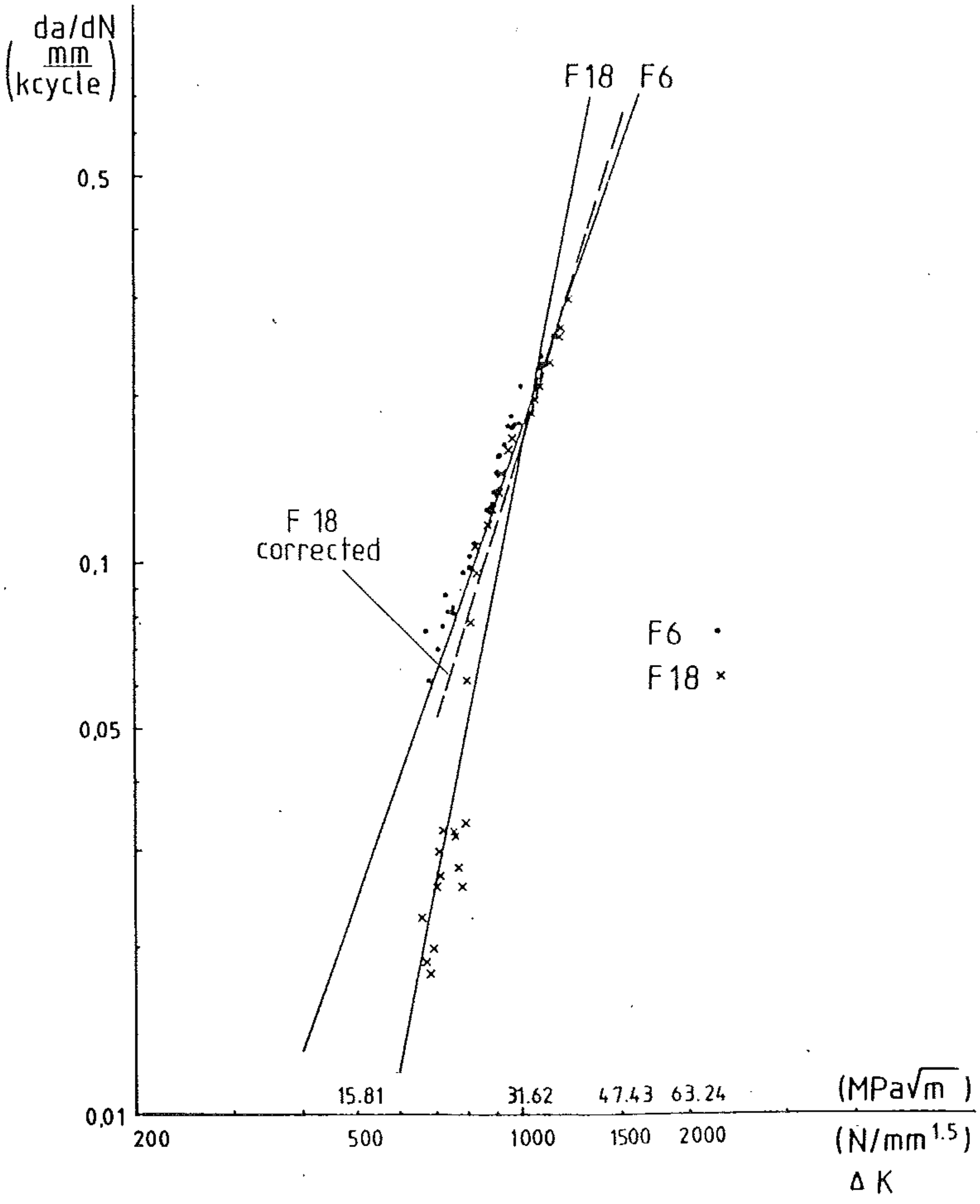

Figure 11. Relationship $da/dN = C(\Delta K)^n$ for specimens F6 and F18

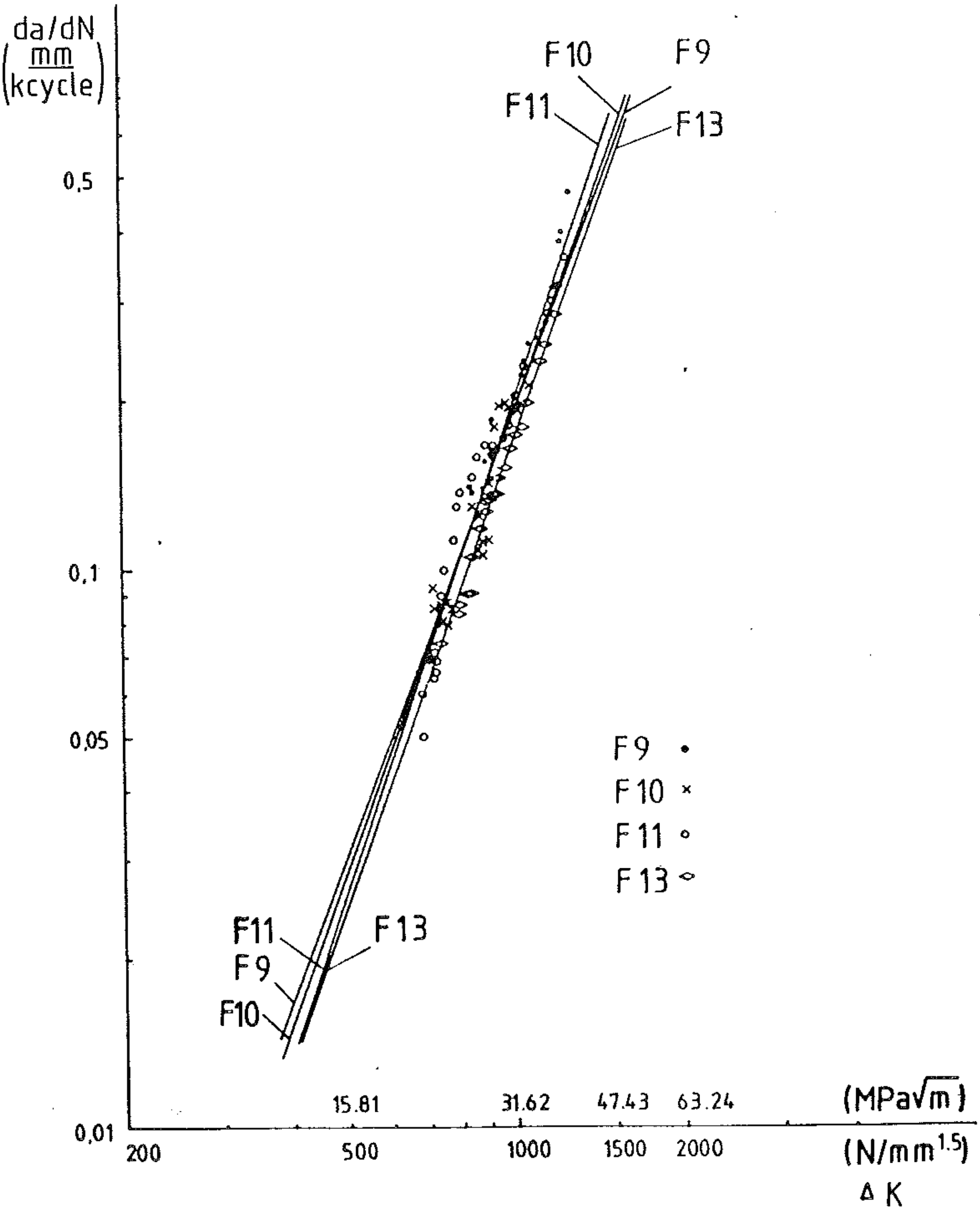

Figure 12. Relationship $da/dN = C(\Delta K)^n$ for specimens F9, F10, F11 and F13

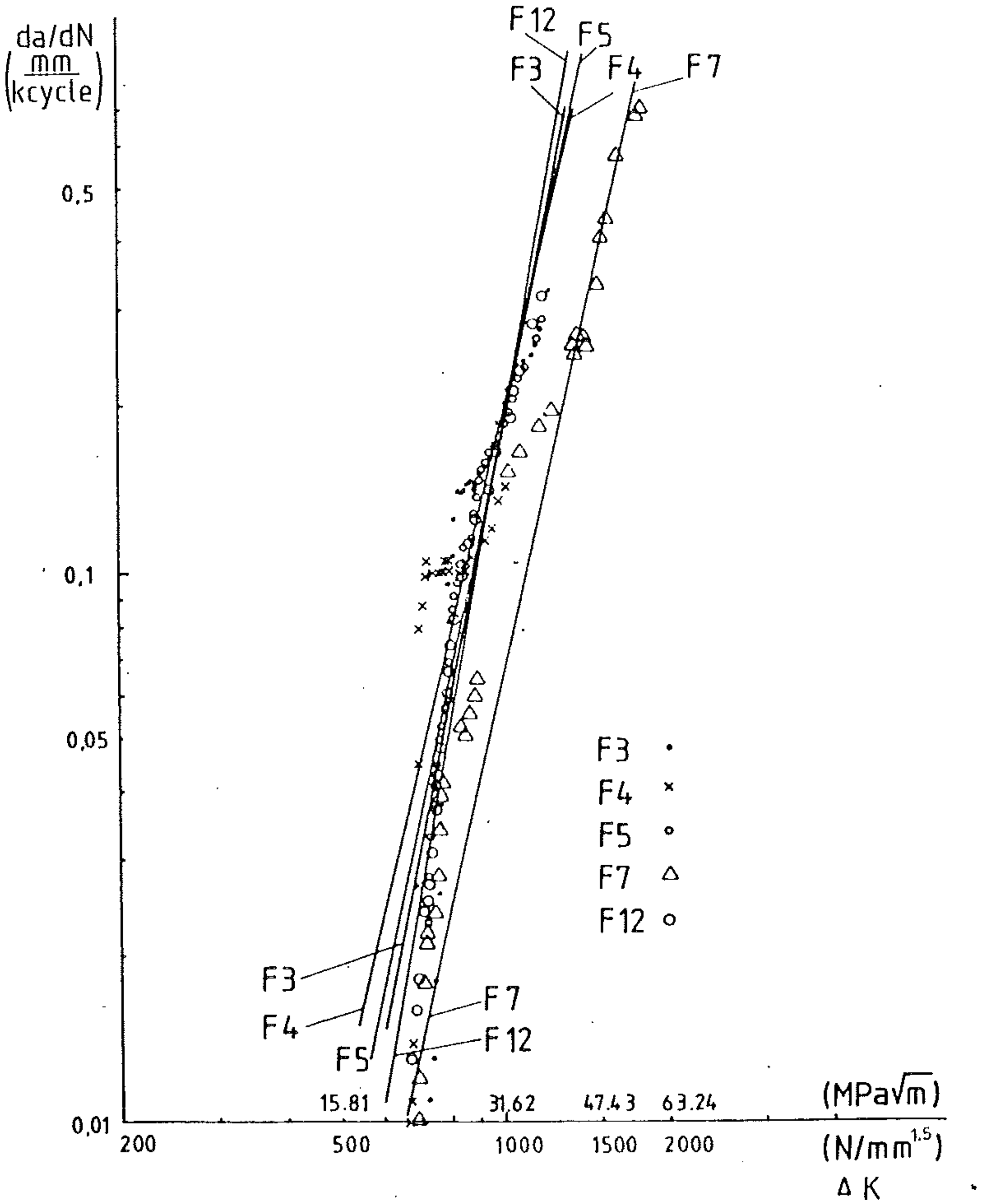

Figure 13. Relationship da/dN = $C(\Delta K)^n$ for specimens F3, F4, F5, F7 and F18

The agreement of results for medium plastic pre-strain level (Fig. 12) is satisfactory. The same can be concluded for the third group of specimens (Fig. 13) with the exception of F7 specimen, exposed to lowest plastic pre-strain.

The final results are listed in Table 5. These results indicate the effect of initial plastic strain in weld metal on crack growth behaviour: lower values of coefficient C and exponent n in Paris law could be attributed to higher level of prior plastic deformation in performed experiment with weld metal of NIONIKRAL 70 Steel.

Table 5. Coefficient C and exponent n in Paris law for differently pre-strained weld metals

Specimen	Initial plastic deformation $\varepsilon_{p\delta}$, (%)	Coefficient C	Exponent n
F6	0.853	1.5098 E -09	2.698
F18	0.874	2.2711 E -09	2.630
F9	0.303	8.5416 E -10	2.794
F10	0.320	1.4365 E -09	2.703
F11	0.467	3.3665 E -10	2.921
F13	0.361	9.7274 E -10	2.746
F3	0.205	2.1289 E -16	4.973
F4	0.100	1.1285 E -13	4.079
F5	0.053	2.6200 E -15	4.612
F7	0.056	4.5798 E -14	4.073
F12	0.109	3.7591 E -18	5.560

Differences in coefficients C and exponents n in Table 5 have to be considered in connection with the relations presented in Fig. 9. For the same loading conditions crack initiated in the specimen with the highest initial plastic deformation at lowest number of cycles and developed to specified length in minimal number of cycles. Immediately after initiation maximal number of cycles was required for the crack growth in specimens with lowest plastic deformation. Results for low stress intensity factor range in Fig. 13 and in Fig. 11 (specimen F18) require further experimental analysis in the region close to treshold behaviour.

Regular shape of a-N curves is obtained for specimens with initial plastic deformation (Fig. 9). This is not the case for specimens in as-welded condition (Fig. 14), tested in similar experiment [4].

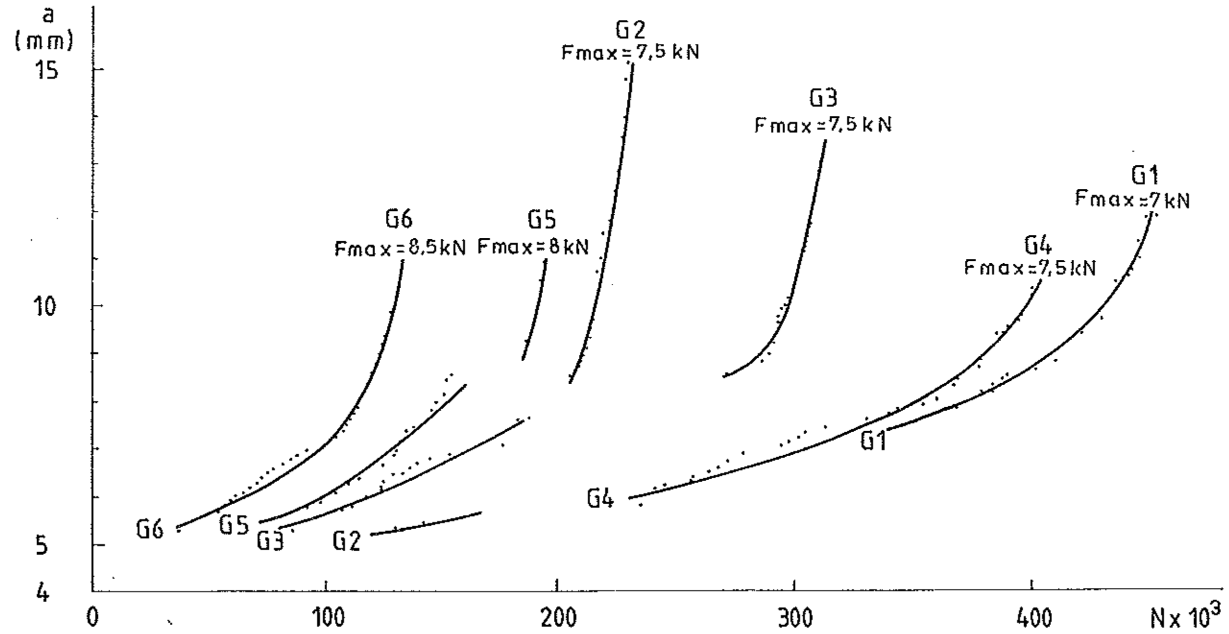

Figure 14. Experimentally obtained a-N relationship of as-welded weld metal exposed to different load ranges with R = 0.1

Irregular behaviour, expressed by pop-ins in some cases, could be attributed to heterogeneity of weld metals or to the existance of defects, which were not discovered in non-destructive testing. The comparison of results from Fig. 9 and Fig. 14 could indicate the beneficial effect of initial plastic deformation in weld metal on its fatigue crack growth behaviour. Possible explanation could be found in blunting effect at the sharp tip of cracks and crack-like deffects, reducing the local stress concentration in these critical regions of weld metal.

CONCLUSION

The experimental results have shown that initial plastic deformation in weld metal (obtained by CO_2 gas shielded welding) of high-strength low-alloyed steel (NIONIKRAL 70) can produce beneficial effects on fatigue crack growth behaviour. This would be of importance for structures in which initial plastic deformation takes place before fatigue loading is applied. However, further investigation is required for better understanding of described relationship and overall behaviour of heterogenious welded joint in fatigue.

ACKNOWLEDGEMENT

This paper is based on work supported by the U.S.-Yugoslav Joint Fund for Scientific and Technological Cooperation, in cooperation with the National Bureau of Standards, Boulder, Colorado under Grant NBS (G) - 755.

REFERENCES

1. Radović, A., Sedmak, S., Nedeljković, Lj.: "Comparative Study of Crack Resistance of Three Differently Alloyed HSLA Steels" in "Mechanical Behaviour of Materials-IV", Proceedings of the Fourth International Conference, Stockholm, Sweden, Pergamon Press, Oxford, 1984, Vol. 2, pp. 919-926

2. Sedmak, S., Radović, A., Nedeljković, Lj.: "The Strength of Welds in HSLA Steel after Initial Plastic Deformation", in "Mechanical Behaviour of Materials-III", Proceedings of the Third International Conference, Cambridge, England, Pergamon Press, Oxford, 1980, Vol. 3, pp. 435-446

3. Božić, B., Sedmak, S., Petrovski, B., Sedmak, A.: "Crack Growth Resistance of Weldment Constituents in a real Structure", to be published in Bulletin SANU

4. Legat, J.: "A Contribution to Crack Growth Investigation of Fatigue Loaded Welded Joints in Structural Steel", Ph. D. Thesys, Faculty of Technology and Metallurgy, University of Belgrade, 1988 (in Serbo-Croatian)

5. ASTM E647-88: Standard Test Method for Measurement of Fatigue Crack Growth Rate, 1988. Annual Book of ASTM Standards, ASTM, Philadelphia, 1988, Vol. 03.01, pp. 636-654

6. Sedmak, S., Petrovski, B.: "The Experimental Analysis for Differently Matched Weld Metals" in Proceedings of The International Conference Joining of Metals JOM-3, Helsingør, Denmark, 1986, pp. 309-313

7. ASTM E399-83: Standard Test Method for Plane-Strain Fracture Toughness of Metallic Materials, 1988 Annual Book of ASTM Standards, ASTM Philadelphia, 1988, Vol. 03.01, pp. 480-504

8. Fuchs, H. O., Stephens, R. I.: "Metal Fatigue in Engineering", John Wiley and Sons, New York, 1980.